Investigation of laser diode face-pumped high average power heat capacity laser

Shenjin Zhang (张申金)[1,2], Shouhuan Zhou (周寿桓)[1,2], Xiaojun Tang (唐晓军)[2], Guojiang Bi (秘国江)[2], and Huachang Lü (吕华昌)[2]

[1]*School of Technical Physics, Xidian University, Xi'an 710071*

[2]*National Key Laboratory of Solid-State Laser, North China Research Institute of Electro-Optics, Beijing 100015*

Received August 10, 2006

The three-dimensional (3D) pump intensity distribution in medium of the laser diode (LD) pumped high average power heat capacity laser is simulated by the ray tracing method, and the divergence characteristics of fast axis and slow axis of LD are simultaneously considered. The transient 3D temperature and stress distributions are also simulated by the finite element method (FEM) with considering the uneven heat source distribution in medium. A LD face-pumped Nd:GGG heat capacity laser is designed. The average output power is 1.49 kW with an optical-optical efficiency of 24.1%.

OCIS codes: 140.3480, 140.6810, 120.6810, 000.4430.

Solid state heat capacity laser is a new concept to solve the problem of waste heat in the medium. In 2004, Rotter *et al.* reported 30-kW laser-diode (LD) pumped heat capacity laser[1−3]. The concept of solid-state heat capacity laser is that during lasing action, waste heat is purposely stored in the medium; during no lasing action, the cooling phase of medium begins[4]. So the surface of medium suffers compressive stress, not tensile stress.

The LD face-pumped Nd:GGG heat capacity lasers are investigated theoretically and experimentally. The average output power was 1.49 kW with an optical-optical efficiency of 24.1%. The three-dimensional (3D) pump distribution in medium is simulated by the ray tracing method and the divergence characteristic of LD is considered synchronously. The transient 3D temperature and stress distribution of medium also are simulated by the finite element method with considering the uneven heat source distribution in medium.

The structure of heat capacity laser is shown in Fig. 1, and the laser propagates along z axis. A $\phi 70 \times 10$ (mm) Nd:GGG of 1.0 at.-% Nd^{3+} doping concentration is used. Every LD array is composed of 33×4 LD bars and four LD arrays are symmetrically placed to pump the end face of medium to obtain even pump distribution. The divergence angles of LD are 3° and 10° in slow and fast axes, respectively. A plano-convex lens with the focus of 200 mm is placed in front of every LD array to compress the pump aperture.

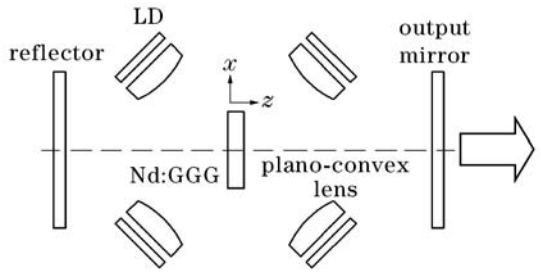

Fig. 1. LD pumped Nd:GGG heat capacity laser.

The pump intensity distribution of end face of medium is shown in Fig. 2. The divergence characteristics of fast axis and slow axis of LD are synchronously considered and the average pump power was 6.19 kW.

Figure 2 shows that the pump intensity distribution is similar to Gaussian distribution along x axis, and the pump intensity distributes homogeneously on the pump area along y axis. The pump intensity distribution of end face of medium $I_{(X,Y)}$ is approximate to

$$I(X,Y) = 1 \times 10^6 \times \exp\left(-\frac{2X^2}{0.03^2}\right)$$

$$\begin{cases} X = [-0.035, 0.035] \\ Y = [-0.02, 0.02] \end{cases}. \tag{1}$$

When the pump propagates along z axis, the heat source distribution $q_v(X,Y,Z)$ in medium can be written as[5]

$$q_v(X,Y,Z) = \eta \times I(X,Y) \times \alpha \times$$

$$\{\exp[-\alpha \times (L/2 - Z)] + \exp[-\alpha \times (L/2 + Z)]\}$$

$$Z = [-0.005, 0.005], \tag{2}$$

where η is the ratio of pump energy converted into heat to all pump energy (in general $\eta \approx 50\%$), α and L are

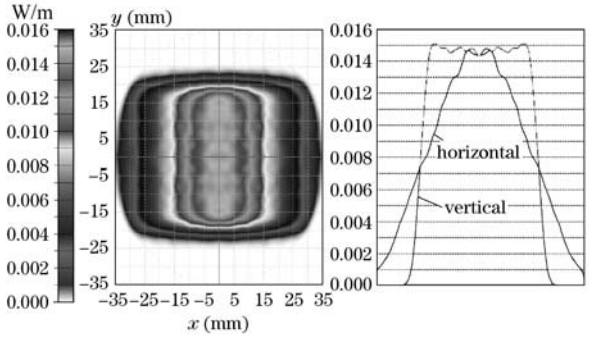

Fig. 2. Pump intensity distribution of end-face Nd:GGG.

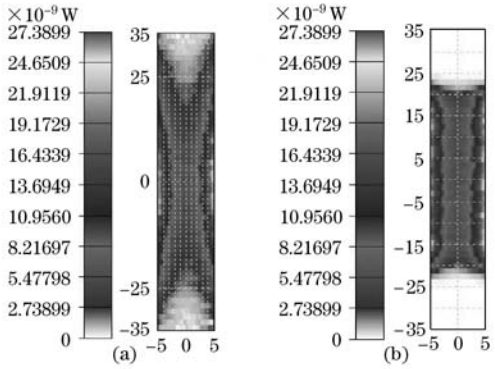

Fig. 3. Pump intensity distribution of x-z plane (a) and y-z plane (b).

the absorption coefficient and the thickness of Nd:GGG, respectively, and the center of medium is the origin of coordinate.

The pump intensity distribution of arbitrary cross-section in medium can be obtained. The pump intensity distributions of x-z plane and y-z plane of medium are shown in Fig. 3, and α is 0.4 mm^{-1}. Along z axis, the pump intensity is high at the center of end face and low at the center of the medium because of the absorption characteristic of medium. Along x and y axes, the pump intensity is higher at the center and lower at the side of medium because of the divergence characteristic of LD. The two factors of absorption of medium and divergence of LD cause the uneven heat source distribution in medium.

The transient heat transfer equation of solid state medium can be written as[6]

$$\frac{\partial T}{\partial t} = \frac{k}{\rho C_p}\left[\frac{\partial^2 T}{\partial r^2} + \frac{1}{r}\frac{\partial T}{\partial r} + \frac{\partial^2 T}{\partial z^2} + \frac{q_v}{k}\right], \qquad (3)$$

where r is the radius, z is the axis orientation, T is the temperature, t is time, k is the heat conduction coefficient, ρ is the density, C_p is the specific heat, and q_v is the heat source density.

The initial temperature of medium is 25 °C, and the side face of medium is weakly restrained so that the medium can expand freely.

The transient 3D temperature and stress distribution of one quarter of medium are shown in Figs. 4 and 5[7]. The lasing lasted 1.2 s and the average pump power was 6.19 kW during the simulation.

Figure 4 shows that the maximum of temperature is 78.1 °C, at the center of end face of medium. The temperature reduces gradually along x axis from the center to the side of medium. Temperature keeps unchanged almost in the most of pump region, and reduces rapidly from pump region to non-pump region along y axis,

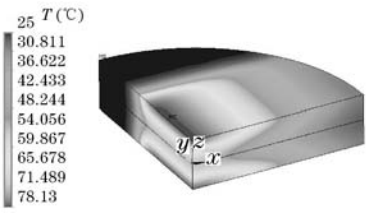

Fig. 4. Temperature distribution of medium.

Fig. 5. Von Mises stress distribution of medium.

because the pump time is short. The temperature is higher on the end face and lower at the center of medium. Those are consistent with pump distribution in medium. Figure 5 shows that the maximum of stress locates at the center of end face of medium, because the heat source intensities here are maximal.

It is obvious that the great temperature gradient complicates the stress distribution in medium. There are compressive stress at the center of end face and tensile stress in the border between pump region and non-pump region, because it is difficulty for the rectangle aperture of pump distribution to match the circular aperture of end face of medium. The large stress restricts the increases of average output power and the lasing time. Key of improving the thermodynamics distribution is to optimize the heat capacity laser.

In the experiment, the pump width of LD was 400 μs. A plano-convex cavity was used, and the transmission of output coupling mirror was 5%. The temperature at the center of end face of medium was 81 °C when the lasing lasted 1.2 s, the average pump power was 6.19 kW, the pump frequency was 500 Hz, and the pump current was 110 A, which is in good agreement with the simulation. Although the maximum temperature increase of 56 °C is lower than 100 °C that heat capacity laser can bear, the working time can be controlled not beyond 1.2 s because the maximum stress of 63.6 MPa in medium is a little larger than safe stress of Nd:GGG (20% of critical stress intensity is 268 MPa).

The average output power and optical-optical efficiency as functions of average pump power are shown in Figs. 6 and 7. During the experiment, the lasing action of heat capacity laser was 0.5 s, and the pump frequency is 100—500 Hz. It is shown that the average output

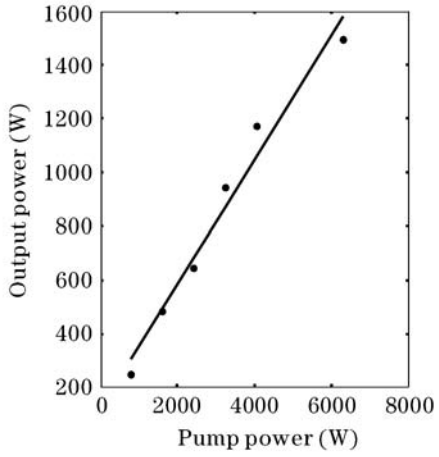

Fig. 6. Average output power versus pump power. Pump pulse width is 400 μs, working time is 0.5 s.

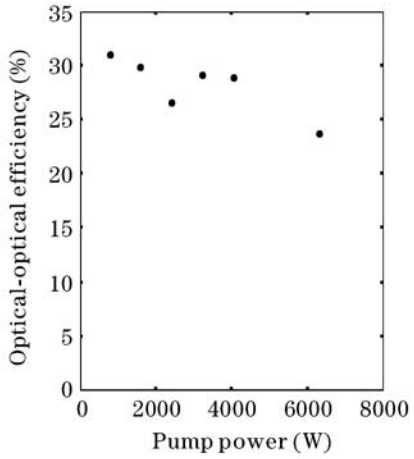

Fig. 7. Optical-optical efficiency versus pump power. Pump pulse width is 400 μs, working time is 0.5 s.

power increases approximatively linearly with the increase of the average pump power. The optical-optical efficiency keeps almost unchanged and just decreases a little when the average pump power increases. That is to say the pump intensity in medium is comparatively lower and the thermal effects are also not obvious when the pump intensity is lower and obvious when the average pump power is higher. The average output power was 1.49 kW with the optical-optical efficiency of 24.1%, when the average pump power was 6.19 kW, the pump frequency was 500 Hz, and the pump current was 110 A.

In this paper, an experimental setup of LD face-pumped Nd: GGG heat capacity laser was designed and the average output power was 1.49 kW with the optical-optical efficiency of 24.1% when the average pump power was 6.19 kW and the lasing time was 0.5 s. The 3D pump distribution in medium is simulated with the ray tracing method, and the transient 3D thermodynamics distribution in medium is also simulated with the finite element method. The simulative and experimental results can be provided to optimize the heat capacity laser as reference.

This work was supported by the Project of National Key Laboratory of Solid-State Laser under Grant No. 413260104. S. Zhang's e-mail address is zhshjin@sina.com.

References

1. C. T. Walters, J. L. Dulaney, B. E. Campbell, and H. M. Epstein, IEEE J. Quantum Electron. **31,** 293 (1995).
2. C. B. Dane, L. Flath, M. Rotter, S. Fochs, and J. Brase, in *Proceedings of 14th Annual Solid-State and Diode Laser Technology Review* 27 (2001).
3. M. D. Rotter, C. B. Dane, S. Fochs, K. L. Fortune, R. Merrill, and B. Yamamoto, Photon. Spectra **38,** (8) 44 (2004).
4. G. F. Albrecht, S. B. Sutton, E. V. George, W. R. Sooy, and W. F. Krupke, Laser and Particle Beams **16,** 605 (1998).
5. A. Yang, D. Chen, J. Wen, S. Wang, D. Cai, and Z. Guo, J. Appl. Opt. (in Chinese) **24,** (4) 23 (2003).
6. Z. Zhao, *Heat Transfer* (in Chinese) (Higher Education Press, Beijing, 2003) p.120.
7. J. Zhao and M. Wang,(eds.) *Elasticity and Finite Elements Techniques* (in Chinese) (Wuhan University of Technology Press, Wuhan, 2003) p.6.